Geometric frustration in the cubic spinels $M\mathrm{Al_2O_4}$ (M=Co, Fe, and Mn)

N. Tristan,[1] J. Hemberger,[1] A. Krimmel,[1] H-A. Krug von Nidda,[1] V. Tsurkan,[1,2] and A. Loidl[1]
[1]*Experimental Physics V, Center for Electronic Correlations and Magnetism, Institute of Physics, University of Augsburg, D-86159 Augsburg, Germany*
[2]*Institute of Applied Physics, Academy of Sciences of Moldova, MD-2028 Chisinau, Republic of Moldova*
(Received 27 May 2005; revised manuscript received 9 August 2005; published 1 November 2005)

X-ray diffraction, magnetic susceptibility, electron-spin resonance, and heat-capacity investigations were performed on $M\mathrm{Al_2O_4}$ compounds with M=Co, Fe, Mn, and Zn. All compounds crystallize in cubic spinel structure AB_2O_4 with minor inversion between A and B sites. $\mathrm{CoAl_2O_4}$ and $\mathrm{FeAl_2O_4}$ reveal spin-glass-like ground states with freezing temperatures well below the Curie-Weiss temperatures indicating strong geometric frustration. Below the freezing temperatures, the heat capacities show a T^2 temperature dependence for $T \rightarrow 0$ K as has recently been observed in some related geometrically frustrated magnets, in contrast to the linear dependence expected for common spin glasses. The heat capacity of $\mathrm{FeAl_2O_4}$ exhibits an additional orbital contribution. With the absence of a cooperative Jahn-Teller distortion, this points toward an orbital freezing. $\mathrm{MnAl_2O_4}$ orders antiferromagnetically below T_N=40 K with a reduced value of the ordered moment and a large paramagnetic component.

DOI: 10.1103/PhysRevB.72.174404 PACS number(s): 75.30.Cr, 75.40.Cx, 76.30.−v, 76.50.+g

I. INTRODUCTION

Geometrically frustrated magnets have generated considerable interest among solid-state physicists. Frustration refers to the inability of a system to satisfy competing interactions giving rise to ground states with a large degeneracy. In contrast to disordered systems, in geometrically frustrated magnets, the spins reside on a well-ordered lattice, but the topology of the structure precludes long-range order. Spins with antiferromagnetic (AFM) interactions on a triangular lattice, or on a three-dimensional network of corner-sharing tetrahedra, known as pyrochlore lattice, are paramount examples. This class of geometrically frustrated magnets[1] exhibits rather complex and fascinating ground states, e.g., like spin liquid[2] or spin ice states.[3,4] Recently, unusual magnetic properties of compounds with spinel structure AB_2O_4 were demonstrated, where geometrical frustration dominates spins residing on octahedral B-sites, forming a lattice equivalent to the pyrochlore structure. Lee *et al.*[5] reported on composite spin degrees of freedom that emerge from frustrated magnetic interactions in cubic $\mathrm{ZnCr_2O_4}$. Furthermore, a number of vanadium spinels reveal rather abnormal properties due to geometric frustration (GF).[6,7] That indeed the B-sites of the spinel lattice are strongly frustrated was outlined almost 50 years ago by Anderson.[8] Recently, it has been shown that normal cubic spinels $\mathrm{FeSc_2S_4}$ and $\mathrm{MnSc_2S_4}$ with only the A-site occupied by magnetic ions also reveal strong GF effects, both in the spin and in the orbital sector.[9–11] Experimentally, geometric frustration of orbitals can be inferred from the observation that a lattice of Jahn-Teller (JT) active magnetic ions does not undergo a cooperative JT transition, as was recently observed in ferrimagnetic $\mathrm{FeCr_2S_4}$,[12] with JT active Fe^{2+} at the A-sites. In this case, the ground state is expected to be an orbital liquid or an orbital glass. In this communication, we present the results of x-ray diffraction, magnetic susceptibility and magnetization measurements, electron-spin resonance, and heat-capacity studies of another group of magnetic spinels, namely, aluminum oxide spinels, also containing only A-site magnetic ions like the above-mentioned sulfide spinels.

In the spinel structure, the A-site ions form a diamond lattice, which can be viewed as two interpenetrating face centered cubic (fcc) sublattices shifted by one quarter along the space diagonal. The exchange interactions between the A-site magnetic ions are complex and involve several interaction paths that are shown in Fig. 1 adopted from Ref. 10. The direct A-A exchange between four nearest neighbors (NN) is ineffective here because of the large distance between the cations (about 3.5 Å). These four NN cations are coupled through six A-O-Al-O-A indirect exchange chains J that include rectangular O-Al-O bonds. The 12 next-nearest neighbors (NNN) cations are coupled through two equivalent A-O-Al-O-A exchange chains J', again including rectangular O-Al-O bonds. The 12 next-next nearest

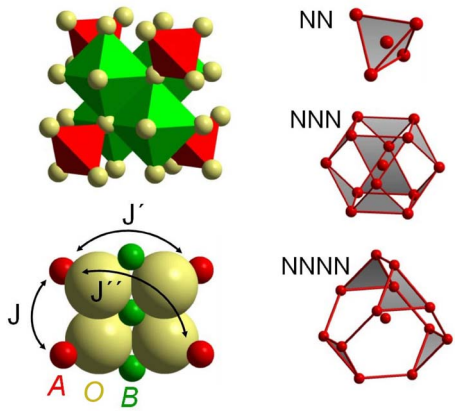

FIG. 1. (Color online) The structure of the AB_2O_4 spinel and the interaction paths between the A-site ions. The A-sites ions (red) are embedded in a tetrahedral environment of oxygen (yellow), while the B sites (green) have octahedral environment (upper left illustration). The right part shows the NN, NNN, and NNNN shells of the A-site lattice.

neighbors (NNNN) cations are coupled through one *A*-O-Al-O-*A* exchange chain J'', including 180° O-Al-O bonds. NNN in the entire sublattice corresponds to the NN within each fcc sublattice. The basic coordination element of the interacting *A*-site ions is the triangle. The coupling within each sublattice is antiferromagnetic and, hence, is frustrated. In addition, both fcc sublattices are coupled again antiferromagnetically, strongly enhancing the frustration effect.[10] Although the interaction between two neighboring *A*-site ions is anticipated to be rather weak, the interaction paths have an extremely high multiplicity explaining the relatively large characteristic (ordering or Curie-Weiss) temperatures observed experimentally.[9,10]

The main scope of the present study is to analyze the effect of different spin and orbital states of the magnetic ions on the ground-state properties within the network of the frustrated spinel lattice in $M\mathrm{Al_2O_4}$ (M=Mn,Fe,Co) compounds. The crystal field at the tetrahedral *A*-site splits the electronic *d* level into a low lying *e* doublet and an upper t_2 triplet. According to Hund's rules, Mn^{2+} ($3d^5$) exhibits a half-filled shell with a total spin $S=5/2$ and zero orbital moment. Fe^{2+} ($3d^6$) has a spin $S=2$ with the orbital moment quenched by the crystal field; however, it is Jahn-Teller active due to the hole in the lower *e* doublet, resulting in residual spin-orbit effects. Finally, Co^{2+} ($3d^7$) has a lower *e* doublet filled by four electrons and a half-filled upper t_2 triplet with $S=3/2$, where spin-orbit effects should be small.

Unusual magnetic properties of $M\mathrm{Al_2O_4}$ compounds are known since 1964, although the type of magnetic order at low temperatures remains an open question. Using susceptibility measurements and neutron powder diffraction, Roth[13] investigated their magnetic structure. In $\mathrm{MnAl_2O_4}$, a collinear antiferromagnetic arrangement of spins similar to that in $\mathrm{Co_3O_4}$ was found below an ordering temperature of 6 K. No long-range magnetic order was detected in $\mathrm{FeAl_2O_4}$, although the magnetic susceptibility reveals a maximum close to 8 K. For $\mathrm{CoAl_2O_4}$, the results were not conclusive, but a long-range ordered state was suggested below 4 K. Later on, neutron diffraction[14] and Mössbauer experiments[15] on $\mathrm{FeAl_2O_4}$ indicated a spin-glass-like transition in this compound.

Our experimental results confirm the long-range order only for $\mathrm{MnAl_2O_4}$, whereas long-range order can be excluded for $\mathrm{FeAl_2O_4}$ and $\mathrm{CoAl_2O_4}$. The latter compounds have spin-glass-like ground states and are characterized by large frustration parameters *f*, as determined from the ratio of the Curie-Weiss to magnetic ordering temperatures, suggesting strong geometrical frustration. In $\mathrm{FeAl_2O_4}$, the tetrahedral Fe^{2+} ions are JT active, but no structural transition indicative of a cooperative Jahn-Teller effect is detected. Consequently, one may speculate that the orbital degrees of freedom are also geometrically frustrated resulting in spin-orbital liquid properties.

II. EXPERIMENTAL DETAILS

Polycrystalline $M\mathrm{Al_2O_4}$ (M=Fe, Mn, Co, and Zn) samples were prepared by solid-state reaction from high purity (99.99% and better) binary oxides (FeO, MnO, $\mathrm{Co_3O_4}$, ZnO, and $\mathrm{Al_2O_3}$) in evacuated quartz ampoules. It is known[14–16] that these compounds at low temperatures have the normal spinel structure with *M* and Al cations predominantly on the tetrahedral *A* and octahedral *B* sites, respectively. At elevated temperatures ($T>500$ °C) some mixing of *M* and Al cations between *A* and *B* sites might occur and the degree of inversion increases with increasing temperature.[16–19] To get the smallest inversion, the synthesis must be performed at the lowest possible temperature but high enough to provide a reasonable diffusion rate. This temperature was found to be approximately 1000 °C. In addition, to facilitate relaxation, all samples were slowly cooled to room temperature with a rate of about 15 °/h. To reach final homogeneity, the synthesis was repeated three or four times. Several batches with the same nominal composition for each ternary compound were prepared. To control the presence of impurity phases, x-ray diffraction, superconducting quantum interference device (SQUID), and electron-spin resonance (ESR) were used. In case of $\mathrm{FeAl_2O_4}$ and $\mathrm{MnAl_2O_4}$, several compositions with excess of FeO and $\mathrm{Mn_3O_4}$ in the range 1–3 mol % were additionally prepared. Samples containing excess of these binary oxides have shown an increased nonlinearity of the magnetization curves (both $\mathrm{FeAl_2O_4}$ and $\mathrm{MnAl_2O_4}$), and noticeable low field magnetization irreversibility ($\mathrm{MnAl_2O_4}$). For $\mathrm{CoAl_2O_4}$ samples, the magnetization nonlinearity and the temperature of the spin-glass-like anomaly were found to correlate with the amount of $\mathrm{Co_3O_4}$ impurity. The most "pure" $\mathrm{CoAl_2O_4}$ sample shows the minimal magnetization nonlinearity and the lowest temperature of the spin-glass-like anomaly. The ESR measurements support this conclusion: The "pure" $\mathrm{CoAl_2O_4}$ sample exhibits the minimal intensity of an additional narrow signal, which appears besides the very broad $\mathrm{CoAl_2O_4}$ resonance line. The intensity ratio between the narrow and broad lines is about 0.4%. The additional ESR signal was identified as belonging to $\mathrm{Co_3O_4}$ impurity by additional measurements of the pure $\mathrm{Co_3O_4}$ phase. Overall, the amount of magnetic impurity phases in ternary magnetic compounds based on the data of the used complementary techniques was estimated to be on the level below 0.5%.

Powder x-ray diffraction was performed utilizing Cu-K_α radiation with a wavelength $\lambda=1.5406$ Å and a position-sensitive detector. A Rietveld analysis was made for all diffraction profiles. The magnetization measurements were done utilizing a commercial SQUID magnetometer Magnetic Property Measurement System (MPMS)-5 (Quantum Design). The heat capacity was measured using a Physical Property Measurement System (PPMS) (Quantum Design) in the temperature range $2\ \mathrm{K}\leqslant T\leqslant 300$ K. ESR studies were performed in a continuous wave mode spectrometer (Bruker ELEXSYS E500) at both *X*-band (9.36 GHz) and *Q*-band (34 GHz) frequencies, equipped with a continuous He gas-flow cryostats (Oxford Instruments) working in the temperature range $4.2\ \mathrm{K}\leqslant T\leqslant 300$ K.

III. EXPERIMENTAL RESULTS AND DISCUSSION

A. X-ray diffraction

Room temperature x-ray diffraction experiments were done on the powdered polycrystalline samples. The diffrac-

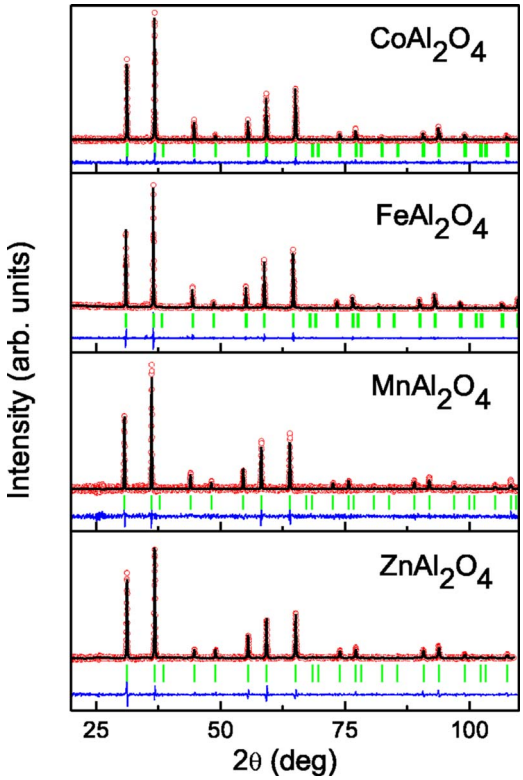

FIG. 2. (Color online) X-ray diffraction profiles of MAl_2O_4. The measured intensities (open circles) are compared with the calculated profile using Rietveld refinement (solid line). Bragg positions of the normal cubic spinel structure are indicated by vertical bars and the difference pattern by the bottom thin solid line.

tion patterns showed a single-phase material for all investigated compounds without any evidence for impurity phases and no residues of nonreacted oxides. Within the Rietveld refinement, 11 parameters have been fitted: scale factor, zero point shift, 3 resolution parameters, lattice parameter, oxygen positional parameter x, inversion parameter δ, and 3 isotropic temperature factors for M, Al, and O, respectively. Representative diffraction profiles for MAl_2O_4, together with the Rietveld refinement and the difference pattern are shown in Fig. 2. The lattice constants a, the oxygen positional parameters x, the inversion parameter δ, and the residuals R are given in Table I.

Lattice parameters and fractional coordinates of oxygen are in rough agreement with the published results.[13,14,16] The x parameters are close to the ideal value 0.25 of the normal

TABLE I. Lattice constants a, oxygen positional parameter x in fractional coordinates (f.c.), cation inversion parameter δ of $(M_{1-\delta}Al_\delta)[Al_{2-\delta}M_\delta]O_4$ compounds, residuals of the refinements R_F, and mean square error Chi^2 as obtained by Rietveld analysis.

Compound	a (Å)	x (f.c.)	δ	R_F (%)	Chi^2
$CoAl_2O_4$	8.1078(3)	0.2611(9)	0.08(3)	4.0	4.0
$FeAl_2O_4$	8.1572(3)	0.2635(4)	0.08(2)	3.8	4.8
$MnAl_2O_4$	8.2246(3)	0.2645(6)	0.06(2)	4.0	4.4
$ZnAl_2O_4$	8.0706(3)	0.2636(4)	0.02(1)	4.6	2.6

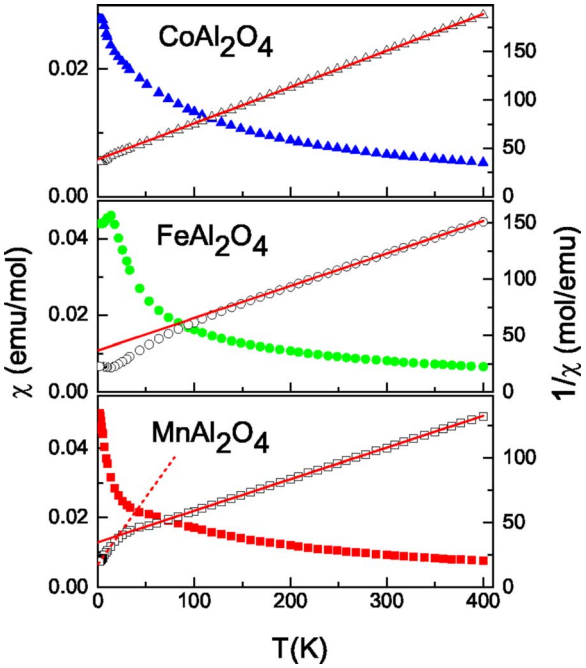

FIG. 3. (Color online) Susceptibility (closed symbols, left scale) and inverse susceptibility (open symbols, right scale) of $CoAl_2O_4$ (upper frame), $FeAl_2O_4$ (middle frame), and $MnAl_2O_4$ (lower frame) vs temperature. The solid lines represent Curie-Weiss fits. In the lower frame, the dashed line indicates a second CW-like law below T_N.

cubic spinel structure. We refined the inversion parameter δ as defined by substitutional disorder according to $(M_{1-\delta}Al_\delta)[Al_{2-\delta}M_\delta]O_4$. The refined inversion parameter is lowest (about 2%) for the Zn and is of the order of 6–8% for the Mn, Fe, and Co compounds, respectively. The inversion parameters for three latter compounds are somewhat smaller than those obtained by Roth,[13] probably due to the lower preparation temperatures of our samples.

B. Magnetic susceptibility and magnetization

Figure 3 presents the temperature dependencies of the molar magnetic susceptibilities χ and of the inverse susceptibilities χ^{-1} for $CoAl_2O_4$ (upper panel), $FeAl_2O_4$ (middle panel), and $MnAl_2O_4$ (lower panel) for temperatures 1.8 K $\leqslant T \leqslant$ 400 K measured in a magnetic field $H=10$ kOe. All compounds exhibit a Curie-Weiss (CW)-like susceptibility at high temperatures. The paramagnetic CW temperature Θ and the effective g value (g_{eff}) were determined from the Curie-Weiss fits to the experimental susceptibility $\chi(T)$ corrected for a diamagnetic contribution χ_{dia}

$$\chi = \chi_{dia} + \frac{\mu_B^2}{3k_B}\frac{g_{eff}^2 S(S+1)}{T-\Theta}. \quad (1)$$

The experimentally observed temperature-independent susceptibility of $ZnAl_2O_4$, $\chi_{dia}=-7.4\times10^{-5}$ emu mol^{-1}, has been taken for all compounds as diamagnetic contribution, in good agreement with the data of Cossee and van Arkel.[20] The resulting fits are indicated as solid lines in Fig. 3. The fit

TABLE II. Spin values, characteristic temperatures, and parameters p_{eff} and Θ determined from the Curie-Weiss fits to the magnetic susceptibilities of $M\mathrm{Al_2O_4}$ spinels. The error presents the deviation between the different batches with the same nominal composition.

	$\mathrm{CoAl_2O_4}$	$\mathrm{FeAl_2O_4}$	$\mathrm{MnAl_2O_4}$
Spin, S	3/2	2	5/2
Curie-Weiss temperature, Θ (K)	−104(2)	−130(1)	−143(5)
Ordering temperature, T_m, T_N (K)	4.8(2)	12(0.5)	40(0.5)
Frustration parameter, $f=\Theta/T_m$	22	11	3.6
Effective moment, $p_{eff}(\mu_B)$	4.65(9)	5.32(3)	5.75(10)
Effective g factor, g_{eff}	2.40(4)	2.17(1)	1.94(6)

parameters, g_{eff} and Θ, and the effective moment $p_{eff}=g_{eff}\mu_B[S(S+1)]^{1/2}$ are listed in Table II. We have neglected temperature-independent van Vleck contributions guided by the fact that they give rise to deviations from the CW law resulting in a negative curvature of the inverse susceptibilities toward high temperatures, which is not observed in our compounds. Both $\mathrm{MnAl_2O_4}$ and $\mathrm{CoAl_2O_4}$ are perfectly described by a CW law down to 50 K and 20 K, respectively. In $\mathrm{FeAl_2O_4}$, the deviations of χ from a CW law are stronger but appear only below 150 K, so that they also cannot be explained by a temperature-independent van Vleck term.

In $\mathrm{CoAl_2O_4}$, the inverse susceptibility is strictly linear for all temperatures, except below 20 K, where χ^{-1} first exhibits a slight downturn and then remains approximately constant below $T_m=5$ K. In $\mathrm{FeAl_2O_4}$, the full paramagnetic moment $p_{eff}=5.32\mu_B$ is observed for $T>175$ K. Below 150 K, χ^{-1} shows an increasing downturn on decreasing temperature yielding a gradual reduction of the effective moment, which may result from orbital fluctuations. At about $T_m=12$ K, χ exhibits a maximum indicating a spin-glass-like freezing. In $\mathrm{MnAl_2O_4}$, the deviation from the high-temperature Curie-Weiss law becomes pronounced on approaching the antiferromagnetic ordering temperature $T_N=40$ K that was deduced from the ESR and specific heat measurements (see Secs. III C and III D), since $\chi(T)$ does not show a maximum at the Néel temperature typically observed in conventional antiferromagnets. Below T_N, the inverse susceptibility χ^{-1} reveals a second Curie-Weiss-like decrease with a strongly reduced effective moment ($2.8\mu_B$) or effective number of spins (25%) and CW temperature (−17 K) in comparison to the high-temperature values, but without any pronounced spin-glass-like anomaly compared to the Co and Fe compounds.

An inspection of Table II reveals that the Curie-Weiss temperature Θ increases with increasing the spin value S, indicating an increase of exchange interactions of the magnetic ions in the paramagnetic regime. The frustration parameter f defined as the ratio of the CW temperature to the long-range magnetic ordering (T_N) or spin-glass (SG) temperature, exceeds a value of 10, both for $\mathrm{CoAl_2O_4}$ and $\mathrm{FeAl_2O_4}$, attributing these compounds to strongly geometrically frustrated magnets.[1] The value of f decreases with increasing spin S and concomitantly with increasing exchange interactions. As intuitively expected, the ordering temperature increases with increasing CW temperature.

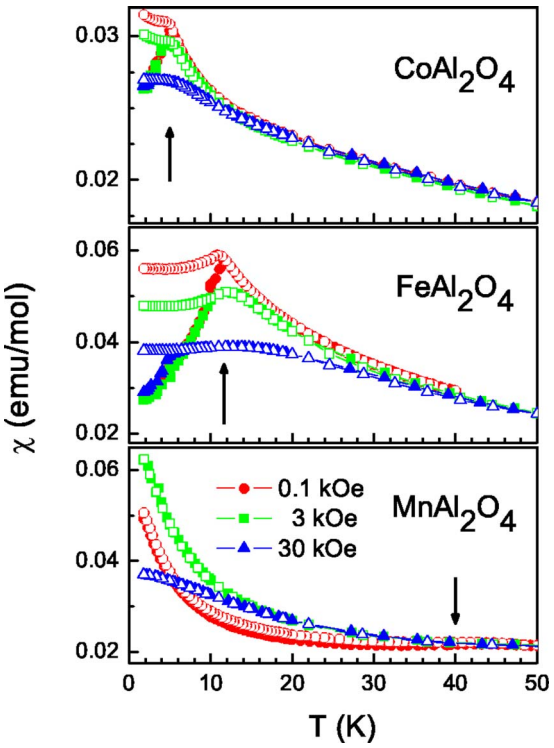

FIG. 4. (Color online) Field-cooled (open symbols) and zero-field-cooled (closed symbols) susceptibilities at different external magnetic fields vs temperature for $\mathrm{CoAl_2O_4}$ (upper frame), $\mathrm{FeAl_2O_4}$ (middle frame), and $\mathrm{MnAl_2O_4}$ (lower frame).

The effective g value is close to 2 for the spin-only system $\mathrm{MnAl_2O_4}$ characterized by a half-filled $3d$ shell, and it is somewhat enhanced for the Fe (~10%) and Co (~20%) aluminum spinels. The enhancement can be understood in terms of spin-orbit coupling corrections to the spin-only value and is typical for Fe^{2+} and Co^{2+} ions in solids.[21]

When comparing our results of the susceptibility analysis shown in Table II with those of Roth,[13] Greenwald *et al.*,[16] and Cossee and van Arkel,[20] we find substantial disagreement for $\mathrm{FeAl_2O_4}$ and $\mathrm{CoAl_2O_4}$. Differences in the effective moments, which are of the order of 10–20%, can be traced back to sample preparation routes and different inversion parameters. The discrepancies are specifically severe for the Curie-Weiss temperatures, which probably result from the susceptibility corrections in the earlier publications. The susceptibility measurements by Greenwald *et al.*[16] and by Cossee and van Arkel[20] have been performed at high temperatures, up to 1000 K and even higher, where the cation inversion strongly increases as a function of temperature, leading to unrealistic high van Vleck contributions at low temperatures. Lotgering's calculations[22] of the van Vleck terms were partly based on the analysis of the measurements of Ref. 20. Roth[13] used these corrections for the analysis of the low-temperature data ($T<300$ K). This probably explains the significantly different CW temperatures for $\mathrm{FeAl_2O_4}$ and $\mathrm{CoAl_2O_4}$. No paramagnetic correction was used in Ref. 13 for the spin-only system $\mathrm{MnAl_2O_4}$ and here the agreement between their Curie-Weiss temperature and our result is quite reasonable.

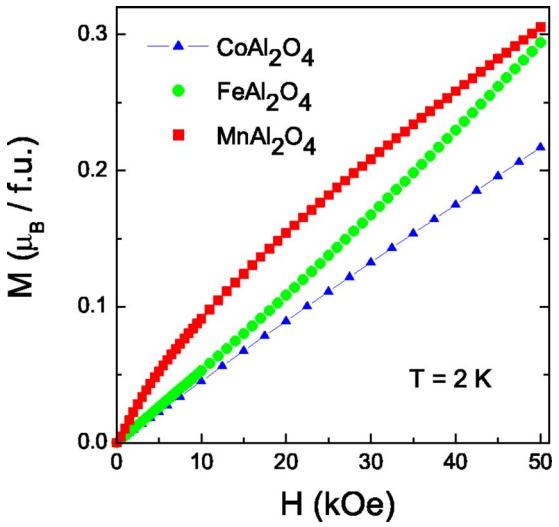

FIG. 5. (Color online) Magnetization vs external magnetic field for MAl_2O_4, M=Co (▲), Fe (●) and Mn (■) at 2 K.

The temperature dependencies of the susceptibilities at different fields in the range around the ordering temperatures are shown in Fig. 4. For $CoAl_2O_4$ and $FeAl_2O_4$, strong differences occur between the zero-field-cooled (ZFC) and field-cooled (FC) susceptibilities indicating spin-glass-like behavior. However, it differs in some aspects from the behavior of canonical spin glasses. For example, the difference between ZFC and FC curves remains still significant up to the highest field (30 kOe), contrary to observations in canonical spin glasses, where low external fields already fully remove the irreversibility.[23] In $MnAl_2O_4$, the low field susceptibility (at H=100 Oe) shows only a marginal difference between ZFC and FC curves below the Néel temperature of 40 K. Contrary to $CoAl_2O_4$ and $FeAl_2O_4$, in $MnAl_2O_4$ both ZFC and FC susceptibilities reveal a pronounced upturn below T_N. This upturn remains qualitatively unchanged for $H<3$ kOe, but becomes suppressed for $H>30$ kOe, probably indicating saturation of a ferromagnetic (FM) component. For this observation below T_N, a canted AFM structure with a small, but still not ordered FM moment seems to be a plausible explanation.

The magnetization curves at 2 K for all three compounds are presented in Fig. 5. In low fields ($H<2$ kOe) M vs H for all samples is close to linear without any noticeable hysteresis. $CoAl_2O_4$ shows a linear dependence of magnetization up to the highest measured field of 50 kOe, while $FeAl_2O_4$ samples reveal a deviation from the linear dependence usually observed for antiferromagnets below the spin-flop field. This effect is small and is visible only at fields above 30 kOe. The nonlinearity of the magnetization is striking for $MnAl_2O_4$ with a clear saturation above 2 kOe. From the magnetization data, we estimated a saturated moment of about $0.05\mu_B$ that may be attributed to about 2.7% of clusters of the B-site Mn ions.[24] This value of inversion is in good agreement with the results of x-ray analysis (Table I). To check the possible presence of a ferrimagnetic impurity phase Mn_3O_4, we measured a $MnAl_2O_4$ sample containing 3% of this binary oxide. The magnetic properties of this mixed composition, however, differ drastically from that of the pure $MnAl_2O_4$ sample. The susceptibility of the mixed composition showed a strong increase below the Curie temperature of 42.5 K of the pure Mn_3O_4 phase. In addition, strong magnetization irreversibility typical for highly anisotropic Mn_3O_4 was immediately detected. X-ray diffraction of the mixed composition also revealed a pronounced (103) peak characteristic of the tetragonal spinel phase Mn_3O_4, which is absent in the original $MnAl_2O_4$ sample. These data definitely exclude the presence of a second phase and relate the high field magnetization behavior of $MnAl_2O_4$ to the saturation of intrinsic paramagnetic clusters due to inversion.

It is important to note that the susceptibility results, which show that a fraction of the manganese moments still remains paramagnetic at low T, as well as the saturating behavior in high fields, suggest that $MnAl_2O_4$ does not adopt a simple collinear antiferromagnetic ground state. Such a structure with each spin on the A sites surrounded by four nearest neighbor A-site ions with opposite spins was proposed by Roth[13] based on the neutron diffraction results. However, the estimate of the ordering temperature T_N of 6.4 K in Ref. 13 to account for a reduced value of the local moment of $3.58\mu_B$ for the Mn ions found at 4 K as compared to $5\mu_B$ expected for a fully ordered spin-only system, disagrees with our experimentally observed value of T_N=40 K (see Table II). Hence, a part of the Mn spins remains paramagnetic and nonordered. This could be due to cation inversion, where A-site and B-site Mn ions build paramagnetic clusters of coupled spins, resulting in a canted AFM structure with a fluctuating ferromagnetic component.

C. Electron-spin resonance

The ESR response of the three aluminum oxide spinels strongly depends on the magnetic A-site ion: $FeAl_2O_4$ turned out to be "ESR silent" confirming the pure Fe^{2+} state of iron, where both the Jahn-Teller and spin-orbit couplings give rise to fast relaxation and, hence, the linewidth is so large that the signal cannot be observed at all. In $CoAl_2O_4$, the ESR signal was obtained at elevated temperatures with a very broad linewidth $\Delta H>10$ kOe, which becomes undetectable below 40 K. The relaxation of Co^{2+}, which is not Jahn-Teller active but is subject to residual spin-orbit coupling, is not so fast as in the Fe compound, but a further useful evaluation of the signal was not possible. Only $MnAl_2O_4$ exhibits well-defined ESR spectra in the whole temperature range.

In Fig. 6 the temperature dependencies of the resonance field H_{res} (lower panel) and linewidth at resonance absorption ΔH (upper panel) as measured at a microwave frequency of 9.36 GHz are presented for $MnAl_2O_4$. In a wide range of temperatures from 300 K to 40 K, the ESR spectrum consists of a single Lorentzian line at a constant resonance field H_{res} yielding a g factor of 1.994(6) typical for Mn^{2+} ions. This g value is in reasonable agreement with that calculated from the susceptibility data. The linewidth increases continuously from 90 Oe at 300 K to 200 Oe at 41 K indicative for the existence of spin fluctuations. On further decreasing temperature, the spectrum broadens and exhibits a substructure typical for a powder pattern in the presence of anisotropy. It can be well described by the su-

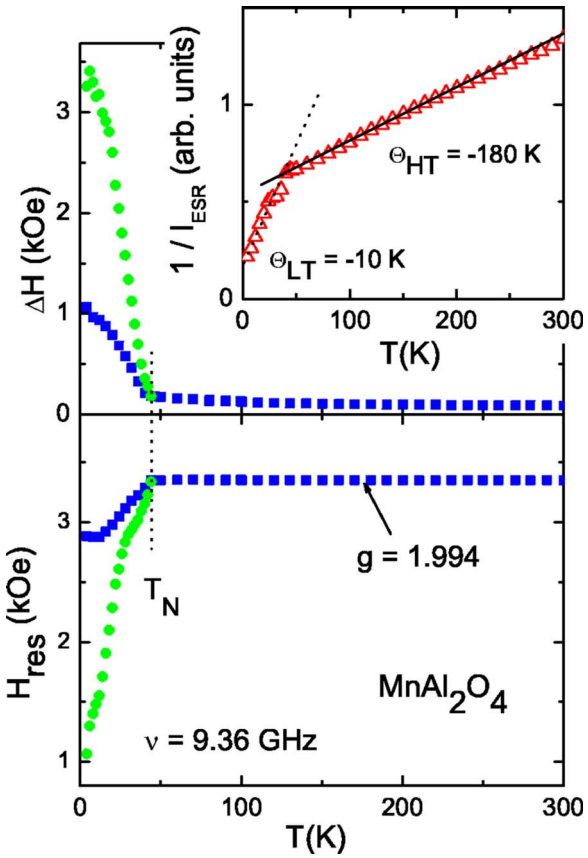

FIG. 6. (Color online) Resonance field H_{res} (lower frame) and linewidth ΔH at resonance absorption (upper frame) as determined in $MnAl_2O_4$ by ESR measurements at X-band frequency. The inset in the upper frame shows the inverse ESR intensity $1/I_{ESR}$ vs temperature. The solid and dotted lines indicate high-temperature and low-temperature CW laws with the corresponding CW temperatures Θ_{HT} and Θ_{LT}.

perposition of two lines of Lorentzian shape. For both of them H_{res} and ΔH exhibit abrupt changes at T_N=40 K, which indicate a transition into a long-range ordered state. Down to T=4 K, the resonance field shifts to H_{res}=2.9 kOe for the narrower line, where the width increases up to ΔH=1 kOe, and to H_{res}=1.0 kOe for the broader line with a maximum width larger than ΔH=3 kOe. The inset in the upper panel shows the inverse ESR intensity vs temperature, which is a measure of the spin susceptibilty. From the high-temperature behavior, we find a CW temperature θ_{HT}=−180 K, somewhat larger than that determined for the bulk susceptibility. Below the AFM ordering temperature, a second Curie-Weiss-like behavior with a CW temperature of θ_{LT}=−10 K is observed, where the slope is increased by a factor of about 6 with respect to the high-temperature law. Comparative ESR measurements at Q-band frequencies (34 GHz) revealed the same constant g value and temperature dependence of the linewidth above T_N as observed in X-band. Below the transition temperature, the qualitative behavior is also the same; however, the resonance shift and broadening of the two components of the spectra are approximately 3–5 times smaller than in the X-band.

The low-temperature data at $T<T_N$ bear puzzling characteristics of both ferromagnetic and paramagnetic resonance.

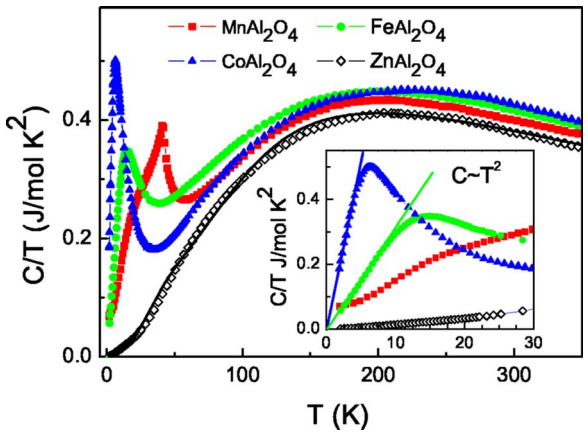

FIG. 7. (Color online) Heat capacities of MAl_2O_4, M=Mn (■), Fe (●), Co (▲), and Zn (◇) plotted as C/T vs T. The inset shows the low-temperature values on an enlarged scale, where the quadratic regime $C\sim T^2$ is indicated by straight lines.

Like the static susceptibility, the Curie-Weiss law of the ESR intensity indicates a paramagnetic contribution either from 1/6 of all spins with full moment of $5\mu_B$ or from all spins with a strongly reduced moment of about $2\mu_B$. The first case would result from the A-B site inversion, which is in rough agreement with the Rietveld refinement of the x-ray diffraction pattern if we take into account that each Mn^{2+} on a B site disturbs six neighboring Mn^{2+} on A sites. In addition, the anisotropy of the ESR spectra cannot be understood in terms of an anisotropic g tensor, because it does not increase linearly with the frequency, but rather decreases with increasing field and frequency. This indicates strong internal fields as in a ferromagnet, where magnetic domains exist at low fields and become reoriented at high fields. These observations suggest a canted antiferromagnetic phase giving rise to the internal fields and domain formation, where the ferromagnetic magnetization component is not long-range ordered, but exhibits quasiparamagnetic properties.

D. Heat capacity

Figure 7 provides an overview of the temperature dependencies of the molar heat capacity C plotted as C/T, for the three magnetic compounds $MnAl_2O_4$, $FeAl_2O_4$, and $CoAl_2O_4$ as well as for nonmagnetic $ZnAl_2O_4$. The data for $FeAl_2O_4$ are in good agreement with that of Klemme and van Miltenburg.[25] At low temperatures, all magnetic compounds exhibit anomalies of the heat capacity related to the onset of magnetic order. $MnAl_2O_4$ shows a well-defined λ anomaly close to 40 K clearly revealing a transition into a long-range ordered state. The heat capacity of $CoAl_2O_4$ and $FeAl_2O_4$ shows maxima at temperatures slightly above the characteristic magnetic ordering temperatures T_m as determined from $\chi(T)$ data indicating spin-glass freezing. It is important to note that in these two SG compounds $C(T)$ approaches 0 strictly following a T^2 dependence (see inset of Fig. 7). In canonical spin glasses the heat capacity shows linear temperature dependence below the cusp observed above the freezing temperature, but a T^2 dependence has also been

TABLE III. Debye and Einstein temperatures estimated from fits to the experimental heat capacities of $M\mathrm{Al_2O_4}$ spinels (see text for detailed explanation).

Compound	Θ_D	Θ_{E1}	Θ_{E2}
$\mathrm{ZnAl_2O_4}$	286	543	1244
$\mathrm{MnAl_2O_4}$	312	522	1092
$\mathrm{FeAl_2O_4}$	310	563	860
$\mathrm{CoAl_2O_4}$	301	530	886

found in geometrically frustrated two-dimensional spin glasses with spinel and distorted Kagomé-based structure.[26,27]

The heat capacity for nonmagnetic $\mathrm{ZnAl_2O_4}$ gives an estimate for the phonon contributions in the total heat capacity of the magnetic compounds. It is known that the primitive unit cell of the spinels contains two formula units giving rise to a total of 42 normal modes.[28] The heavy Zn ions are mainly responsible for the low-energy motions (<360 K) whereas Al and O ions are involved in vibrational modes over a wide range of energies and the total phonon density of states in $\mathrm{ZnAl_2O_4}$ spans up to about 1200 K.[29] Hence, for a reasonable description of the phonon spectrum of the spinels, a combined Einstein-Debye model should be employed, where $C(T)$ is defined by expression[30]

$$C(T) = 3Ra_0x_D^{-3}\int_0^{x_D}\frac{x^4e^x}{(e^x-1)^2}dx + R\sum_{i=1}^{s-1}a_i\frac{x_{E_i}^2e^{x_{E_i}}}{(e^{x_{E_i}}-1)^2}. \quad (2)$$

The first term in (2) represents the Debye heat capacity related to the acoustic modes, and the second term is a sum of Einstein phonon contributions related to optic modes. Θ_D and Θ_E are Debye and Einstein temperatures, respectively, x_D and x_E are reduced inverse temperatures, defined via $x_D=\Theta_D/T$ and $x_E=\Theta_E/T$. The constants a_i indicate the numbers of degrees of freedom for each contribution. The parameter $s=7$ denotes the number of atoms per formula unit and $R=8.31$ J mol^{-1} K^{-1} is the molar gas constant.

In the temperature range from 2 K to 350 K, the temperature dependence of the heat capacity of $\mathrm{ZnAl_2O_4}$ can be reasonably fitted (solid line in Fig. 7) using Eq. (2), with a Debye temperature $\Theta_D=286(15)$ K, Einstein temperatures $\Theta_{E1}=543(50)$ K and $\Theta_{E2}=1244(100)$ K, and the 21 lattice degrees of freedom distributed according to $a_0:a_1:a_2=3:12:6$, i.e., three acoustic degrees of freedom, and the remaining 18 optic degrees of freedom distributed among 2 Einstein oscillators. The Debye temperatures for $M\mathrm{Al_2O_4}$ (M=Mn, Fe, and Co) were evaluated using a method proposed in Ref. 31, taking into account the different atomic masses of $\mathrm{ZnAl_2O_4}$ and of the magnetic compounds $M\mathrm{Al_2O_4}$. The Einstein temperatures were obtained from the fits to the experimental data for each compound in the temperature range above 100 K, 200 K, and 50 K for $\mathrm{MnAl_2O_4}$, $\mathrm{FeAl_2O_4}$, and $\mathrm{CoAl_2O_4}$, respectively, where deviations from the Curie-Weiss law are minimal. The values of the Debye and Einstein temperatures used for the analysis are summarized in Table III.

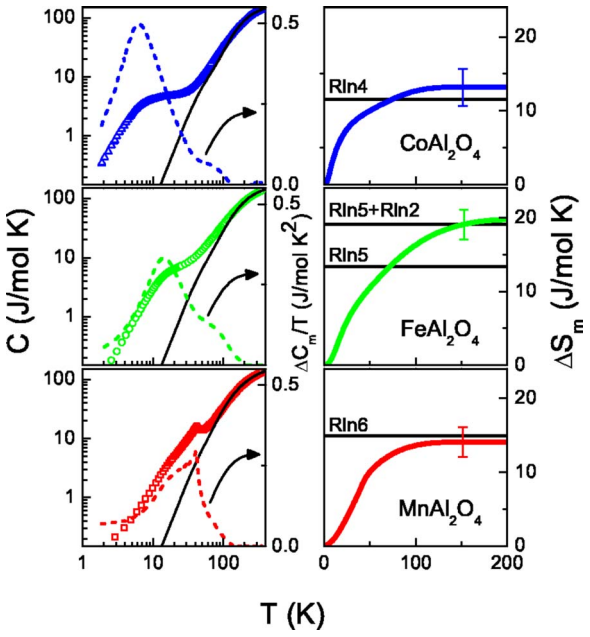

FIG. 8. (Color online) Left row: Heat capacities of $\mathrm{CoAl_2O_4}$ (upper frame), $\mathrm{FeAl_2O_4}$ (middle frame), and $\mathrm{MnAl_2O_4}$ (lower frame) vs temperature (left scale). The solid lines characterize the phonon contributions. Also shown (dashed lines) are the purely magnetic contributions $\Delta C_m/T$ to the heat capacity. Right row: Calculated magnetic entropies ΔS_m of $\mathrm{CoAl_2O_4}$ (upper frame), $\mathrm{FeAl_2O_4}$ (middle frame), and $\mathrm{MnAl_2O_4}$ (lower frame). The vertical bars show the error in the entropy calculation at high temperatures due to the error in fitting of the phonon contribution.

The observed heat capacities for the magnetic compounds are replotted in the left row of Fig. 8 on a double logarithmic scale where the calculated phonon contributions are presented by solid lines (left scale). After subtraction of the phonon contribution, the calculated magnetic contributions ΔC_m to the heat capacity are also shown in the left row of Fig. 8 as $\Delta C_m/T$ (right scale). The magnetic contributions reveal maxima close to the characteristic ordering temperatures. In canonical spin glasses a peak in C vs T is usually observed at 1.3 T_m.[23] In the Co and Fe compounds, however, the peak appears at about 2 T_m. The additional shoulders in $\Delta C_m/T$ observed around 80 K for $\mathrm{FeAl_2O_4}$ and $\mathrm{CoAl_2O_4}$ possibly correspond to low-lying phonon modes, since our fitting model employs only two Einstein modes.

The magnetic entropy $\Delta S_m(T)$ was calculated according to

$$\Delta S_m(T) = \int_0^T \frac{\Delta C_m(T)}{T}dT. \quad (3)$$

The estimated entropies for each compound are shown in the right row of Fig. 8. For $\mathrm{FeAl_2O_4}$ and $\mathrm{CoAl_2O_4}$, at the SG transition, the magnetic entropy is considerably smaller than theoretically expected for the spin degree of freedom. This indicates that a significant fraction of the entropy is released already at high temperatures, a clear signature of geometrical frustration. For $\mathrm{MnAl_2O_4}$, the magnetic entropy is in agreement with the theoretical spin-only value of $R\ln(6)$ for $\mathrm{Mn^{2+}}$ ions at tetrahedral coordination. The value of the magnetic

entropy for $CoAl_2O_4$ is slightly enhanced compared to $R\ln(4)$ expected for a $S=3/2$ system with quenched orbital moment. This small excess of magnetic entropy indicates that the upper maximum observed in the magnetic heat capacity at 80 K could be related to a low-lying phonon mode. Another possible explanation, which is based on the x-ray results, takes into account a small part of Co^{2+} ions on the *B* sites which are JT active and might additionally contribute to the heat capacity.

The most intriguing result which comes from the specific heat study is that the entropy for $FeAl_2O_4$ is significantly higher than the theoretical spin value. It certainly cannot be explained by a small inversion (of about 4%) and, hence, by a presence of the Fe^{2+} ions at the *B* sites. It is evident that the orbital degrees of freedom have to be taken into account, yielding a total entropy of $R\ln(5)$ for the $S=2$ spin contribution plus $R\ln(2)$ for the orbital contribution of the Jahn-Teller active *e* doublet. This value comes close to the entropy as experimentally observed in $FeAl_2O_4$ at high temperatures.

IV. CONCLUDING REMARKS

The experimental investigation of the structural, magnetic, and thermodynamic properties of a number of ternary aluminum oxides MAl_2O_4, with M=Co, Fe, Mn, Zn, testify several important peculiarities. The magnetic ions with partly filled 3*d* shell are located predominantly on the tetrahedrally coordinated *A* sites of the cubic spinel structure. $CoAl_2O_4$ and $FeAl_2O_4$ reveal high magnetic frustration parameters of 22 and 11, respectively. Despite the fact that these are almost chemically ordered compounds, they possess spin-glass-like ground states. Comparing their field-cooled and zero-field-cooled magnetic susceptibilities with that of paramount examples of geometrically frustrated magnets, like the normal spinel $AlCr_2O_4$ with magnetic ions on the *B* sites,[26] or $SrCr_8Ga_4O_{19}$ compound,[27] we find striking similarities. The same is true for the low-temperature specific heat in $Fe(Co)Al_2O_4$, which strictly follows a T^2 dependence toward zero temperature. In the Sr-Cr-Ga oxide, this fact has been explained in terms of a two-dimensional character of the antiferromagnetic excitations. In the normal spinels, the concept of two-dimensionality, however, can hardly be justified and the T^2 dependence of the specific heat must be of another origin. Theoretical studies[32] predict such a dependence for Jahn-Teller glasses. In this context, one may consider that the Fe^{2+} ion in a tetrahedral crystal field is Jahn-Teller active. In $FeAl_2O_4$, the magnetic specific heat reveals an additional contribution related to the orbital degree of freedom, but the JT effect is suppressed and at the lowest temperatures, this compound can be viewed as a spin-orbital liquid. It is similar to the spin-orbital liquid observed recently in the related spinel compound $FeSc_2S_4$, which also manifests a T^2 dependence of the specific heat as T approaches 0.[9] It has been stated already, a long time ago, by Goodenough[33] that for the tetrahedral-site Fe^{2+}, any static crystalline distortion is strongly influenced by long-range elastic coupling. This is consistent with the recent observations that in $FeCr_2S_4$, the cooperative JT effect, which appears close to 10 K, can be easily suppressed by marginal disorder resulting again in a T^2 dependence of the specific heat.[12] Taking into consideration the observed T^2 dependence, $FeAl_2O_4$ can be viewed as spin-orbital liquid near glassy freezing as well.[10] In $CoAl_2O_4$, this remains an open question, but it may result from local strain due to residual spin-orbital coupling.

In $MnAl_2O_4$, we found an unconventional long-range antiferromagnetic ground state. Below 40 K, a canted antiferromagnetic configuration is suggested, but with a remaining fluctuating ferromagnetic component. From the ESR and susceptibility measurements, we found that this fluctuating moment is of the order of $2\mu_B$, which roughly corresponds to the missing value of the ordered moment of the antiferromagnetic structure. No further magnetic transition could be detected down to 2 K. A pronounced magnetic saturation in high fields provides further experimental support for this scenario.

From a more general point of view, it seems necessary to explain the Curie-Weiss temperatures of the order of 100 K, which were observed in all studied magnetic compounds, and to give an estimate of the exchange couplings in these *A*-site spinels. As outlined before, the exchange along a single path between two neighboring *A*-site magnetic ions is rather weak as it always involves three intermediate nonmagnetic ions (Al-O-Al). Roth[13] has discussed these superexchange paths and they have been further elucidated in Refs. 9 and 10. The exchange paths between the nearest and the next-nearest neighbors involve intermediate Al-O-Al ions and exhibit a multiplicity of 24 each. The exchange path between next-next-nearest neighbors have a multiplicity of 12. Although these neighboring shells are at various distances in real space, the length of the exchange paths is not significantly different. In a rough approximation, one can assume the equal strength of all three exchange integrals. Then, a simple mean-field estimate of the interaction $J/k_B = 3\Theta/[2zS(S+1)]$ with the number of interacting neighbors $z=60$, and $S=2$ and $\Theta=100-140$ K, yields a value $J/k_B = 0.4-0.7$ K for the magnetic exchange per interaction path between a pair of *A*-site magnetic ions, which is reasonable regarding the comparable values in related compounds.[34]

Summarizing, our magnetic and specific heat studies demonstrate that *A*-site magnetic aluminum oxide spinels reveal clear signs of geometrical frustration both in spin and orbital degrees of freedom. These results confirm the earlier suggestions of Ref. 9 that strong geometric frustration effects are indeed a universal property of normal spinels with only the *A*-site occupied by magnetic ions.

ACKNOWLEDGMENTS

This work was supported by the Deutsche Forschungsgemeinschaft via the Sonderforschungsbereich 484 (Augsburg) and partly by Bundesministerium für Bildung und Forschung (BMBF) via VDI/EKM, FKZ 13N6917. The support of U.S. Civilian Research and Development Foundation and Moldovan Research and Development Association (MRDA) is gratefully acknowledged.

[1] A. P. Ramirez, in *Handbook of Magnetic Materials*, edited by K. H. J. Buschow (Elsevier Science, Amsterdam, 2001), Vol. 13, p. 423.
[2] B. Canals and C. Lacroix, Phys. Rev. Lett. **80**, 2933 (1998).
[3] A. P. Ramirez, A. Hayashi, R. J. Cava, R. Siddhartan, and B. S. Shastry, Nature (London) **399**, 333 (1999).
[4] S. T. Bramwell and M. J. P. Gingras, Science **294**, 1495 (2001).
[5] S-H. Lee, C. Broholm, W. Ratcliff, G. Gasparovic, Q. Huang, T. H. Kim, and S-W. Cheong, Nature (London) **418**, 856 (2002).
[6] O. Tchernyshyov, Phys. Rev. Lett. **93**, 157206 (2004).
[7] M. Reehius, A. Krimmel, N. Büttgen, A. Loidl, and A. Prokofiev, Eur. Phys. J. B **35**, 311 (2003).
[8] P. W. Anderson, Phys. Rev. **102**, 1008 (1956).
[9] V. Fritsch, J. Hemberger, N. Büttgen, E-W. Scheidt, H-A. Krug von Nidda, A. Loidl, and V. Tsurkan, Phys. Rev. Lett. **92**, 116401 (2004).
[10] N. Büttgen, J. Hemberger, V. Fritsch, A. Krimmel, M. Mücksch, H-A. Krug von Nidda, P. Lunkenheimer, R. Fichtl, V. Tsurkan, and A. Loidl, New J. Phys. **6**, 191 (2004).
[11] A. Krimmel, M. Mücksch, V. Tsurkan, M. Koza, H. Mutka, and A. Loidl, Phys. Rev. Lett. (to be published).
[12] R. Fichtl, V. Tsurkan, P. Lunkenheimer, J. Hemberger, V. Fritsch, H-A. Krug von Nidda, E-W. Scheidt, and A. Loidl, Phys. Rev. Lett. **94**, 027601 (2005).
[13] W. L. Roth, J. Phys. (Paris) **25**, 507 (1964).
[14] J. L. Soubeyroux, D. Fiorani, E. Agostinelli, S. C. Bhargava, and J. L. Dormann, J. Phys. (Paris) **49**, Suppl. 12, C8-1117 (1988).
[15] J. L. Dormann, M. Seqqat, D. Fiorani, M. Nogues, J. L. Soubeyroux, S. C. Bhargava, and P. Renaudin, Hyperfine Interact. **54**, 503 (1990).
[16] S. Greenwald, S. J. Pickart, and F. H. Grannis, J. Chem. Phys. **22**, 1597 (1954).
[17] L. Larsson, H. St. C. O'Neill, and H. Annersten, Eur. J. Mineral. **6**, 39 (1994).
[18] R. J. Harrison, S. A. T. Redfern, and H. St. C. O'Neill, Am. Mineral. **83**, 1092 (1998).
[19] A. Nakatsuka, Y. Ikeda, Y. Yamasaki, N. Nakayama, and T. Mizota, Solid State Commun. **128**, 85 (2003).
[20] P. Cossee and A. E. van Arkel, J. Phys. Chem. Solids **15**, 1 (1960).
[21] S. Krupička, *Physik der Ferrite und Verwandten Magnetischen Oxide* (Academia Verlag der Tschechoslovakischen Academie der Wissenschaften, Prague, 1973).
[22] F. K. Lotgering, J. Phys. Chem. Solids **23**, 1153 (1962).
[23] J. A. Mydosh, *Spin Glasses: An Experimental Introduction* (Taylor and Francis, London, 1993).
[24] G. Srinivasan and M. S. Seehra, Phys. Rev. B **28**, 1 (1983).
[25] S. Klemme and J. C. van Miltenburg, Am. Mineral. **82**, 68 (2003).
[26] K. Matsuno, T. Katsufuji, S. Mori, M. Nohara, A. Machida, Y. Moritomo, K. Kato, E. Nishibori, M. Takata, M. Sakata, K. Kitazawa, and H. Takagi, Phys. Rev. Lett. **90**, 096404 (2003).
[27] A. P. Ramirez, G. P. Espinosa, and A. S. Cooper, Phys. Rev. Lett. **64**, 2070 (1990).
[28] A. Chopelas and A. M. Hofmester, Phys. Chem. Miner. **18**, 279 (1991).
[29] C. M. Fang, C-K. Loong, G. A. de Wijs, and G. de With, Phys. Rev. B **66**, 144301 (2002).
[30] E. S. R. Gopal, *Specific Heats at Low Temperatures*, edited by K. Mendelssohn and K. D. Timmerhaus (Heywood Books, London, 1966).
[31] M. Bouvier, P. Lethuillier, and D. Schmitt, Phys. Rev. B **43**, 13137 (1991).
[32] M. A. Ivanov, V. Y. Mitrofanov, L. D. Falkovskaya, and A. Y. Fishman, J. Magn. Magn. Mater. **36**, 26 (1983).
[33] J. B. Goodenough, J. Phys. Chem. Solids **25**, 151 (1964).
[34] F. K. Lotgering, J. Phys. (Paris) **32**, Suppl. 12, C1-34 (1971).